Geophysical Research Letters

RESEARCH LETTER
10.1029/2020GL087456

Key Points:
- Hydrography and simple dynamics are combined to examine temporal characteristics of Nordic Seas MOC
- An approximately ±10–15% range in mass and heat transport into the Nordic Seas in synchrony with the Atlantic multidecadal variability
- There is no evidence for long-term trend in transport toward the Nordic Seas

Supporting Information:
- Supporting Information S1

Correspondence to:
T. Rossby,
trossby@uri.edu

Citation:
Rossby, T., Chafik, L., & Houpert, L. (2020). What can hydrography tell us about the strength of the Nordic Seas MOC over the last 70 to 100 years?. *Geophysical Research Letters*, *47*, e2020GL087456. https://doi.org/10.1029/2020GL087456

Received 10 FEB 2020
Accepted 22 MAY 2020
Accepted article online 30 MAY 2020

What can Hydrography Tell Us About the Strength of the Nordic Seas MOC Over the Last 70 to 100 Years?

T. Rossby[1], Léon Chafik[2], and Loïc Houpert[3]

[1]Graduate School of Oceanography, University of Rhode Island, Kingston, RI, USA, [2]Department of Meteorology and Bolin Centre for Climate Research, Stockholm University, Stockholm, Sweden, [3]National Oceanographic Centre, European Way, Southampton, UK

Abstract The flow of warm water into the Nordic Seas plays an important role for the mild climate of central and northern Europe. Here we estimate the stability of this flow thanks to the extensive hydrographic record that dates back to the early 1900s. Using all casts in two areas with little mean flow just south and north of the Greenland-Scotland Ridge that bracket the two main inflow branches, we find a well-defined approximately ±0.5 Sv volume transport (and a corresponding ±30 TW heat flux) variation in synchrony with the Atlantic multidecadal variability that peaked most recently around 2010 and is now trending down. No evidence is found for a long-term trend in transport over the last 70 to 100 years.

Plain Language Summary Society has been much concerned about the possibility of the slow-down of what is popularly known as the Gulf Stream and its transport of warm water to high latitudes of the North Atlantic. Were this to happen it is generally understood that the climate of central and northern Europe would turn distinctly colder. Direct measurements of the warm water flow toward the Nordic Seas and cold water flowing back into the deep North Atlantic show no change over the last couple of decades. To reach further back in time we have considerable information about the hydrographic state of the North Atlantic and Nordic Seas since the early 1900s. By examining the difference in sea level between the North Atlantic and Norwegian Sea we find a ~70-year variation in volume and heat transport that is clearly associated with the Atlantic multidecadal variation. It peaked most recently around 2010 and is now trending down. We note that the Atlantic multidecadal variation accounts for the observed variations so well we find no evidence for a longer-term increase or decrease in transport.

1. Introduction

The flow of warm water north into the northern North Atlantic is a major distinguishing feature of the Atlantic (Buckley & Marshall, 2016). As it flows north it releases heat to the atmosphere keeping the winds comparatively warm to far higher latitudes than any other ocean basin (e.g., Palter, 2015). This flow north is known as the upper branch of the meridional overturning circulation (MOC). As it flows and loses heat it becomes increasingly dense such that when the water crosses the meridian between Cape Farewell, Greenland, and Scotland a process of branching and transformation takes place along which water leaves the upper ocean to feed and join the lower south-flowing branch of the MOC (Chafik & Rossby, 2019). The partitioning of the upper branch is such that roughly half leaves the surface in the Subpolar North Atlantic and turns south at intermediate depths (what one might call the shallow overturning branch) while the other half continues north hereafter referred to as the Nordic Seas MOC where very dense water is produced and pooled behind the Greenland-Iceland-Faroe-Scotland Ridge (Chafik & Rossby, 2019; Dickson et al., 2008; Hansen & Østerhus, 2000). This dense water spills back into the deep North Atlantic between Greenland and Scotland as the deep overturning branch of the MOC. It is a slow-down or collapse of this Nordic Seas branch of the MOC that has been cause for concern (e.g., Broecker, 1997). The shallow branch may be quite variable (e.g., Lozier et al., 2019), but there is no evidence that it can shut down as the deep branch has (e.g., McManus et al., 2004) given that it was quite active even during the last glacial period (e.g., Curry & Oppo, 2005).

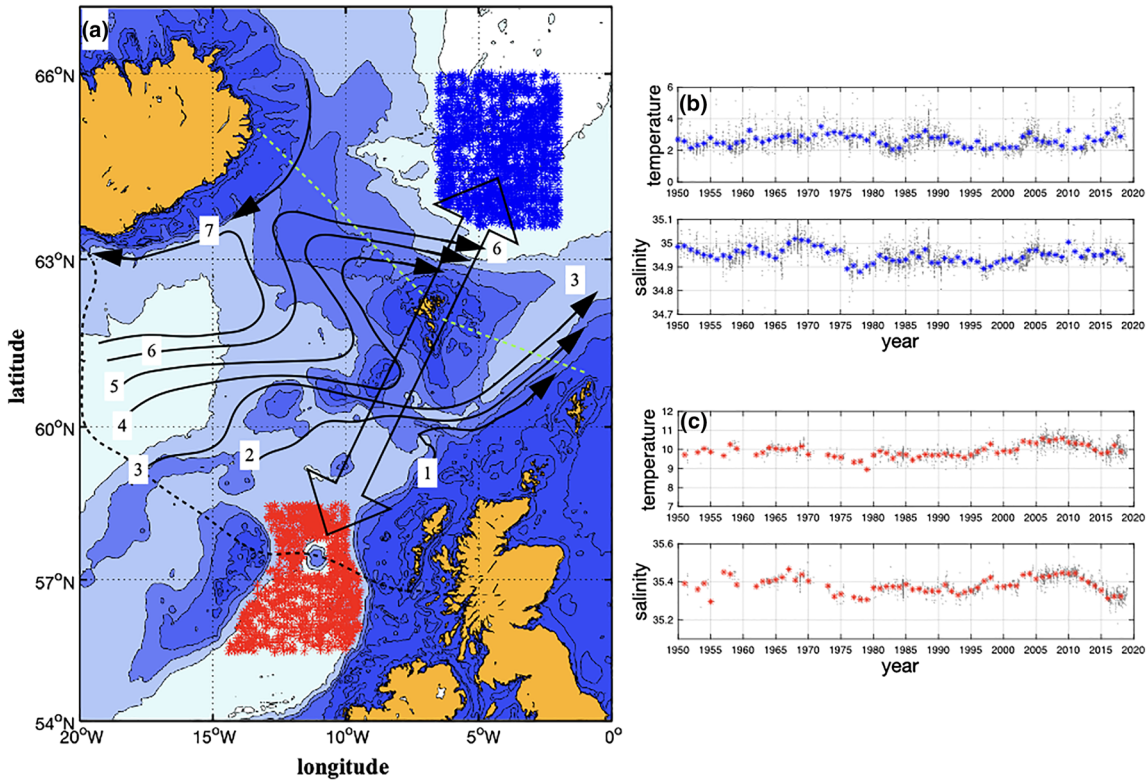

Figure 1. (a) The blue and red dots show all hydrocasts in the southern Norwegian Sea and Rockall Trough used in this study. The two regions span both warm water pathways into the Nordic Seas indicated by the transport contours (Childers et al., 2015). Bathymetric contours at 200, 500, 1,000, 2,000, and 3,000 m. Dashed green lines show the Norröna route across the Faroe-Shetland Channel and along the Iceland-Faroe Ridge. Dashed black line shows extended Ellet line (Holliday et al., 2015). The right panels (b) and (c) show 0–500 m deseasoned average temperature and salinity data and their annual averages (stars) for the Norwegian Sea (blue) and Rockall Trough (red).

Several programs have been in place over the last 2–3 decades to measure overflow from the Nordic Seas into the deep North Atlantic (e.g., Hansen et al., 2016; Jochumsen et al., 2017) while others have focused on flow toward the Nordic Seas (e.g., Berx et al., 2013; Hansen et al., 2015; Rossby et al., 2018). Here we attempt to expand the window backward in time by using hydrographic data since the early 1900s to provide insight into how transport toward the Nordic Seas may have trended or varied since the dawn of modern oceanography. The approach taken is to assemble all hydrographic data from two regions that bracket both the IFR and FSC inflows to estimate the dynamic height difference between two regions. This difference, assuming geostrophy, can be used to determine transport given a velocity reference, which we can obtain from the Norröna program (Rossby et al., 2018).

2. Methods and Data

2.1. Hydrography

The chart in Figure 1 shows the two principal upper ocean (0–400 m) transport pathways according to Childers et al. (2015), one passing through the FSC and the other across the IFR. The basis for the following analysis is that this upper ocean inflow into the Nordic Seas must be in geostrophic balance with the difference in sea level between the northeast Atlantic and the southern Nordic Seas, an assumption that will be validated later. To estimate this difference, two quiet areas bracketing the two pathways will be defined. By quiet we mean both little mean flow and low eddy activity; the former to avoid aliasing estimates of transport and the latter to improve estimates of interannual variability. The regions are the Rockall Trough (RT) and the southern Norwegian Sea (NS), respectively (Figure 1a). In the supporting information (Text S1) we describe the organization and processing of the data in further detail.

The standard dynamic method is used to estimate geostrophic transport (Fofonoff, 1962). This approach gives us total transport between the two regions without regard to or knowledge of how it might be partitioned into the IFR and FSC branches. As will be seen the assumption of geostrophy works well for the inflow, but not for the overflow.

We begin with the standard definition of dynamic height anomaly ΔD:

$$\Delta D = \int_0^p \delta \, dp, \tag{1}$$

where δ, the specific volume anomaly, is defined as $\delta = \alpha(S, T, p) - \alpha_0$ and $\alpha_0 = \alpha(35, 0, p)$ is the specific volume at local pressure with $S = 35$ and $T = 0°C$.

Average geostrophic velocity normal to the line separating the two stations relative to the surface is then

$$v(p) = -f^{-1}(\Delta D_b(p) - \Delta D_a(p))/(x_b - x_a) + v_0, \tag{2}$$

where $(x_b - x_a)$ is the horizontal distance ($dist$) between the two stations and v_0 is an arbitrary integration constant with dimension velocity. It is set = 0 at the surface. Total transport relative to the surface is obtained by integration of velocity and multiplied by distance:

$$T_{b-a}(p) = dist \int_0^p v(p) \, dp = -f^{-1} \int_0^p dp \int_0^p (\delta_b - \delta_a) \, dp. \tag{3}$$

Transport relative to a nonzero pressure p (or depth) can be obtained by setting an offset velocity v_0 to the integral such that $v(p) = 0$. This was common practice in earlier oceanographic studies where it was assumed that the ocean at depth was nearly motionless. Today, directly measured currents and/or satellite-measured sea surface tilt can be used to reference the dynamic method (next sections). The unit of transport is 1 Sv (erdrup) = 10^6 m^3 s^{-1}.

2.2. Velocity

To calibrate the hydrographic estimates of transport, this study uses the 2009–2016 average velocity field through the FSC and across the IFR (Rossby et al., 2018). These absolute velocity data were obtained from an ADCP mounted in the hull of the high-seas ferry Norröna, which operates on a weekly schedule from the Faroes to Denmark and Iceland.

2.3. Altimetry

Monthly mean values of sea surface height (SSH) from the DUACS DT2018 multimission satellite altimetry (Taburet et al., 2019) are utilized to study the sea level trends and variability for the RT and southern NS areas in Figure 1. We use the 1/4° monthly mean absolute dynamic topography (the sum of sea-level anomalies and the MDT_CNES/CLS 2013 ocean mean dynamic topography) between January 1993 and December 2018 (Chafik et al., 2019). As with hydrography, yearly averages of SSH give us a single time series of sea level variability for the two regions.

3. Results and Discussion

3.1. Validating the Dynamic Method With Satellite Altimetry

Dynamic height measures the expansion or contraction of a water column due to density change (the δ in Equation 1 is the inverse of density). As a water column warms it expands and sea level rises. It is the ability to measure these variations accurately that has made satellite altimetry so powerful. It also has excellent spatial coverage. This gives us a means for checking whether the far fewer hydrographic stations within the predefined regions can still capture their low-frequency variability. Figure 2a shows SSH variations since 1993. These two time-series are constructed exactly the same way as for hydrography: for each month for the entire 1993–2018 record, average SSH is computed for the two areas (the black dots). These are then deseasoned resulting in the thin red and blue lines, respectively. Averaging the SSH records year-by-year yields the annual time series, the thick lines. A linear fit to these yields the sea level rises indicated in the figures, almost all of which represents global sea level rise (Cazenave et al., 2018). The variations around these trends represent variations in dynamic height due to the Atlantic

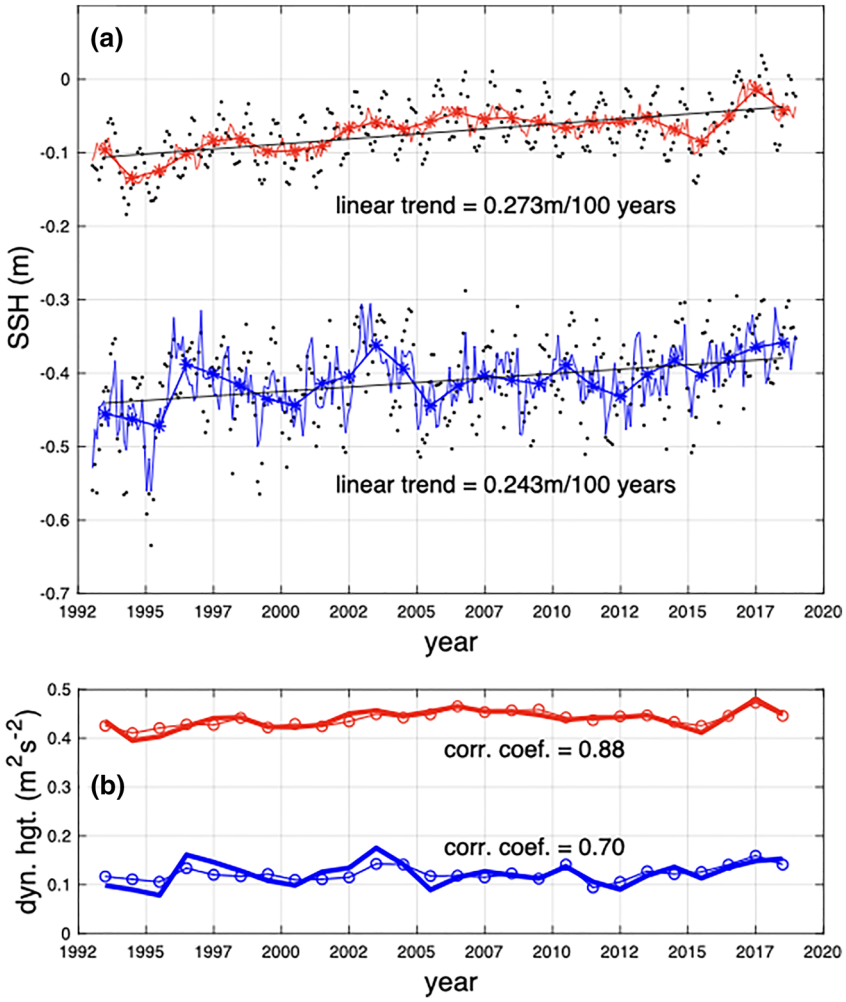

Figure 2. (a) Satellite altimetric sea surface height (SSH) for RT and NS. The dots represent monthly averages, the thin red and blue lines the deseasoned time series and the heavy lines the annual averages. The thin black lines are the linear trends. (b) Surface to 500 m dynamic height (line and circles) for RT (red) and NS (blue) and detrended SSH from altimetry (solid line) superimposed. The panel shows the correlation coefficients between the two.

multidecadal variability (AMV) and effects of winds especially in the NS (Chafik et al., 2019). Figure 2b compares dyn. hgt between 0 and 500 m estimated using Equation 1 and SSH after removing the common sea level rise. The correlation coefficient between the two annual series is 0.7 and 0.88 for the NS and RT series, respectively, a satisfactory validation of our approach to pool hydrographic data to increase degrees of freedom for estimating transport variability.

3.2. Dynamic Height Anomaly and the Dynamic Method

Our starting points are the temperature and salinity data sets for the two regions, Figures 1a and 1b. Using Equation 1 the corresponding 0–500 dbar (or meter) dynamic height anomaly (ΔD) data sets including all data from before 1950 can be estimated (Figure 3a). (For the purposes of this study 1 dbar = 1 m.) Figure 3b shows the casts available for each year for the two regions. Starting around 1950 the data volume increases substantially, but there are scattered data from the beginning of the 1900s that will be used. The difference in dynamic height between the two regions can be used to determine velocity (Equation 2) and transport (Equation 3). But to do so we need to determine v_o in Equation 2 so that the transports have the proper magnitude. Fortunately, we know the absolute transport for the 2009–2016 period well thanks to the Norröna operation (Rossby et al., 2018). We proceed in two steps: First, determine the mean

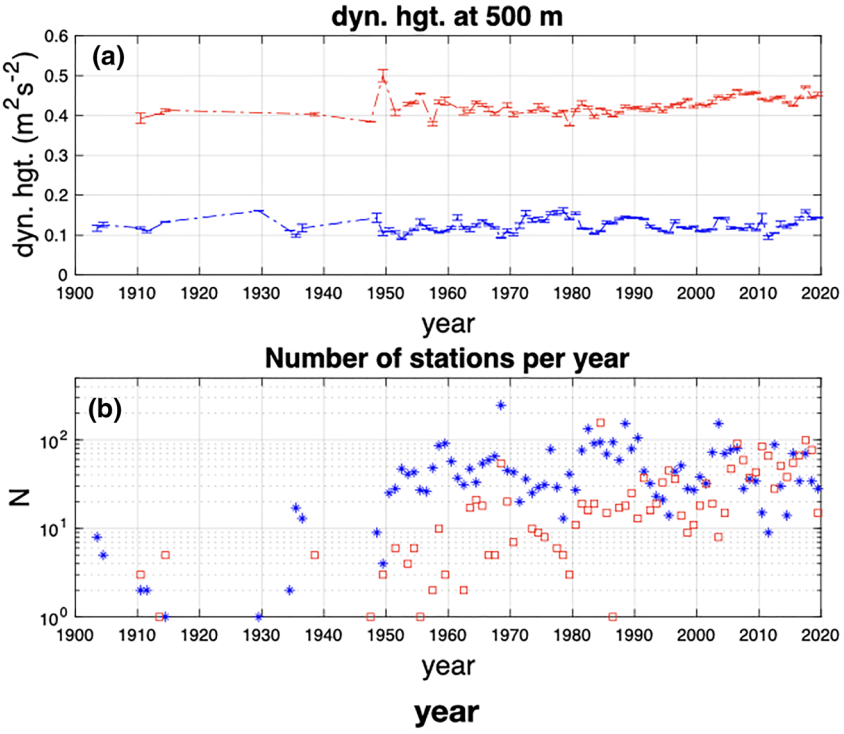

Figure 3. (a) Annual average and standard error for 0–500 m dynamic height as a function of time since 1900 for the two regions (red for RT, blue for NS). The very high dynamic height in 1949 (RT) is due to three casts taken in or near a very warm eddy. (b) Number of casts available per year. There are 4,201 and 2,804 casts for the two regions, respectively.

geostrophic velocity profile for the same 2009–2016 period. Second, use the Norröna velocity data to determine at what depth the velocity goes to/through zero. Figure 4a shows the ΔD integrals for the two regions for the 2009–2016 period. The difference between these two gives geostrophic velocity from the surface according to Equation 2 (dashed line). The next step is to determine the reference velocity v_o. The green curve shows the 8-year average velocity profile for the 2009–2016 period from the Norröna (obtained from Rossby et al., 2018). It passes through 0 m s^{-1} at 489 m at which depth the dynamic height difference = 0.31 dyn. m. We reinterpolate the geostrophic profile to 1 m resolution and shift it so

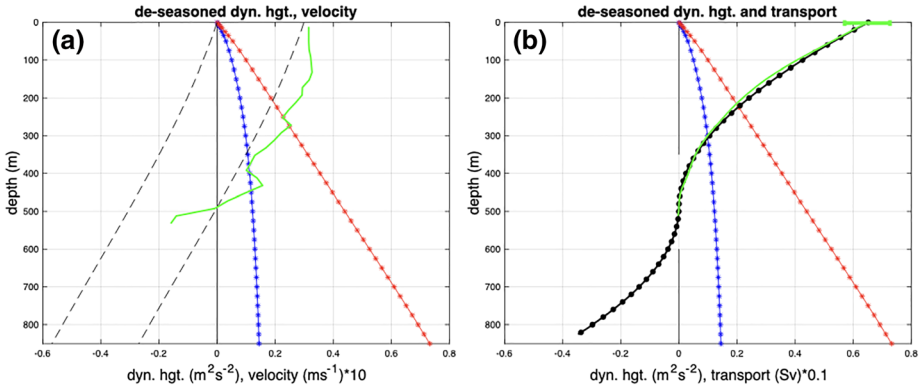

Figure 4. (a) Dynamic height and geostrophic velocity starting at the surface and shifted right (dashed lines) so it goes through zero at 489 m. The green curve shows the 8-year average velocity from the Norröna ADCP sections. (b) The corresponding integrated geostrophic and directly measured transports. Note the ±0.8 Sv uncertainty (taken from Rossby et al., 2018).

it equals zero at 489 m (dashed line shifted right) such that $v_o = 0.03$ m s^{-1} at the surface. Whereas the geostrophic velocity is based on a nominal 821 km distance between the two regions, the measured profile is the 8-year average of all water passing through the IFR and FSC. The irregularity of the velocity profile reflects the decreasing width of the two openings from 770 km at the surface to 300 km at 500 m depth (see bathymetry in Figure 1a).

Integrating the adjusted geostrophic velocity and directly measured mean velocity profiles (Equation 3) leads to the transport profiles shown in Figure 4b. The error bar in ADCP transport is dominated by the lack of degrees of freedom for the large IFR contribution to transport (Rossby et al., 2018). In comparison, the uncertainty in the geostrophic estimate is far smaller due to the O(200) hydrocasts available from this period for averaging. The geostrophic profile does not include a ~0.6 Sv flow north along the Scotland Slope (estimated from numerous lowered ADCP velocity profiles across the Scotland slope along the Extended Ellet Line, Figure 1). But the objective here is to establish a reasonable mean profile around which to study variability. Rossby et al. (2018) and Østerhus et al. (2019) give the best estimates for mean exchange between the North Atlantic and the Nordic Seas. For the rest of the paper we will use 500 m as the reference depth for transport estimates. This is held constant since a similar calibration or depth determination at times past is not possible. The deep overflow (flow in the opposite direction at depth) is discussed in the supporting information (Text S2).

3.3. Temporal Change

The key step of this paper is to use the dynamic height records to determine geostrophic transport in the past. Figure 5a shows estimated annual mean transport for nearly every year since 1950. What is most striking about this figure is the roughly ±0.5 Sv variation in transport on interdecadal time scales. These are principally due to changes in heat content in RT, the principal contributor dynamic height change as the interannual-to-decadal variations have a different character in the NS and RT (Figures 5b and 5c). A strong relationship can be seen between transport and temperature fluctuations in RT ($R = 0.8$) and less so for that with temperature in NS ($R = -0.37$). This points to the northeast Atlantic as the source of the observed transport variations. More specifically, it points to the AMV as a primary contributor to transport variability. Figure 5d superimposes transport on a composite AMV index based on two different data sets (HadISST and ERSST) and two approaches (Trenberth & Shea, 2006; van Oldenborg et al., 2009) that essentially remove the global mean sea-surface temperature from those of the North Atlantic Ocean. The agreement is good since 1950 when data coverage improves, but even the few data points from the early 1900s fit the fluctuations associated with the AMV: a peak in transport in the 1940–1950 range, a minimum around 1980 and a maximum 2010 with a downturn developing since then (Frajka-Williams et al., 2017). Just as important, the overall agreement between estimated transport and the AMV is such that any residual trend is so small that based on Figure 5d we cannot be sure of its sign and conclude therefore that there is no evident long-term trend over the instrumental record.

3.4. Heat Transport Variations

Heat transport (H) varies with volume transport (V) and an average temperature (T). An estimate of how much H varies (H') is given by

$$H' = <V> T' + V' <T>, \tag{4}$$

where T represents an average temperature. Given a 0.5 Sv amplitude to the transport (V') and a corresponding 0.5°C temperature amplitude (T', Figure 1, lower right) $H' = 6.2$ Sv × 0.5°C × C_p + 0.5 Sv × 9°C × C_p, where C_p is the heat capacity (4×10^6 Jm^{-3}°C^{-1}) = $(12.4 + 18) \times 10^{12}$ W, i.e., ±30 TW. Given that the 270 TW heat transport reported by Rossby et al. (2018; see also Segtnan et al., 2011) was estimated when transport was near a maximum and is now down-trending, this suggests that heat flux may decrease to perhaps ~210 TW in the coming decades if the AMV pattern persists. Such a large variation in heat transport accords with studies that have noted warm and cold phases with lesser and greater ice coverage in the Barents Sea (Årthun et al., 2012; Boitsov et al., 2012; Smedsrud et al., 2013). It is worth noting that while the instrumental record (from 1870–present) of the AMV only spans two cycles there is some evidence for its existence over the last millennium (Wang et al., 2017; Zhang et al., 2019).

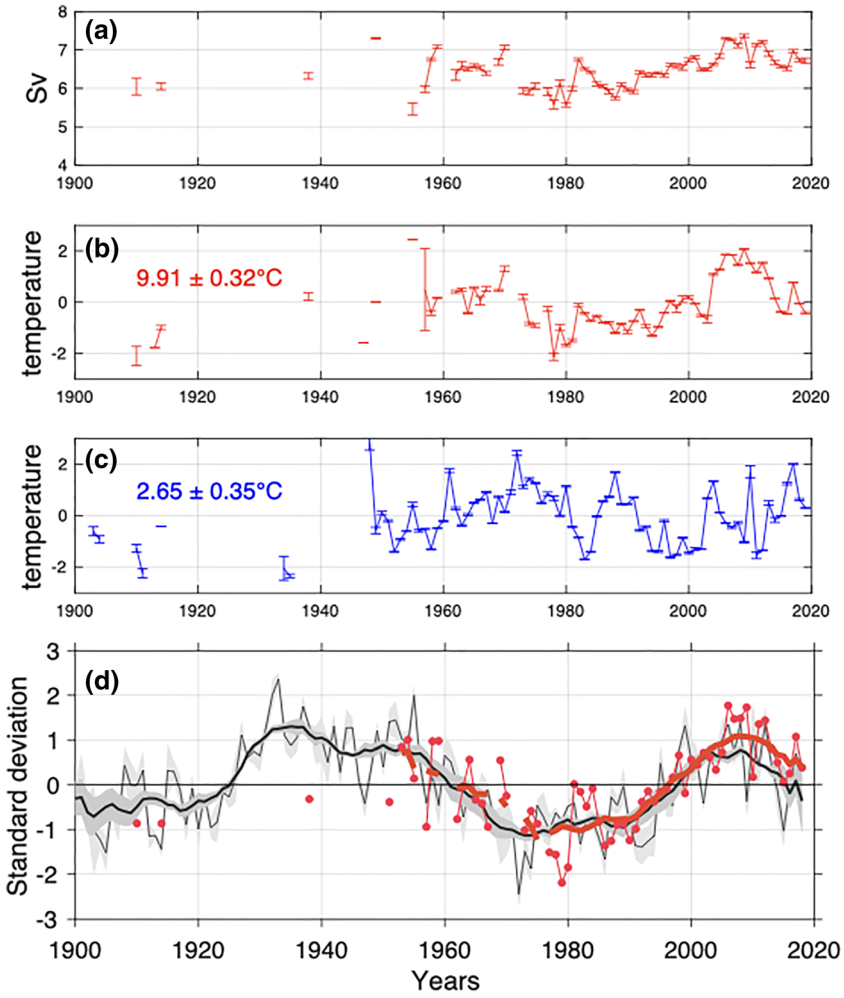

Figure 5. (a) Annual averages of baroclinic transport assuming a constant level of no motion at 500 m depth (top panel). The middle panels (b) and (c) show normalized temperature variability for Rockall Trough and Norwegian Sea using the mean and standard deviations indicated in color. The bottom panel (d) superimposes annual (light) and 11-year (heavy) standardized and low-pass filtered transport variability (red) and AMV index (black). The AMV is an ensemble mean of four different indices calculated based on two different definitions (Trenberth & Shea, 2006, and van Oldenborg et al., 2009) and two data sets (HadISST and ERSST). The definition by Trenberth and Shea (2006) subtracts the global mean sea-surface temperatures (60°S–60°N) from those of the Atlantic Ocean (0–80°W, 0–60°N). The definition by van Oldenborg et al. (2009), however, omits the tropical region, averages sea-surface temperatures north of 25°N (7–70°W, 25–60°N) and subtracts the regression on global mean temperature. The dark (light) gray shaded area is the standard deviation based on the low-pass filtered (annual) AMV indices.

4. Summary

By combining a variety of hydrographic casts from regions with little mean flow in the northeast Atlantic and southern NS one can construct a record of dynamic height difference that measures transport of all warm water entering the Nordic Seas. This time series reveals a significant variation in both volume and heat transport that is clearly linked to the AMV. The agreement between transport and the AMV is noteworthy for two reasons. First, there is evidence for a distinct ~70-year variation superimposed with maxima centered around 1940 and 2010 with a downturn developing in recent years (Frajka-Williams et al., 2017). Second, the fit is so good or tight that we cannot identify any longer-term residual trend that can be credibly bound away from zero. While this finding that both volume and heat transport vary in synchrony with the AMV has no predictive value, the absence of a measurable longer-term trend suggests a stable Nordic Seas heat flux. This is, at least for now, contrary to the apprehension of a persistent slow-down of the MOC (Broecker, 1997).

Acknowledgments

This study is an extension of work on inflow into the Nordic Seas based on the Norröna project funded by the U.S. National Science Foundation, support for which is gratefully acknowledged. It took shape during the first author's visits to the International Meteorological Institute at the University of Stockholm. L. C. acknowledges support through the Swedish National Space Agency (Dnr 133/17) and the FiNNESS project. L. H. is supported by the UK-OSNAP-Decade National Environmental Research Council (NERC) grant NE/T00858X/2. The early hydrographic data come from the ICES Dataset on Ocean Hydrography managed by the International Council for the Exploration of the Sea, Copenhagen. 2014. The later UDASH data are available from the PANGAEA data archive. The digital open access data library PANGAEA is a publisher for earth system science and hosted by the Alfred Wegener Institute. UDASH is stored in 36 ASCII *.txt files (one file for each year; https://doi.pangaea.de/10.1594/PANGAEA.872931) (Behrendt et al., 2018). We thank P. Holliday and a second reviewer for their excellent comments and suggestions. These have materially improved this manuscript.

References

Årthun, M., Eldevik, T., Smedsrud, L. H., Skagseth, Ø., & Ingvaldsen, R. B. (2012). Quantifying the influence of Atlantic heat on Barents Sea ice variability and retreat. *Journal of Climate*, *25*, 4736–4743.

Beaird, N. L., Rhines, P. B., & Eriksen, C. C. (2013). Overflow waters at the Iceland–Faroe Ridge observed in multiyear seaglider surveys. *Journal of Physical Oceanography*, *43*(11), 2334–2351. https://doi.org/10.1175/JPO-D-13-029.1

Behrendt, A., Sumata, H., Rabe, B., & Schauer, U. (2018). UDASH – Unified database for Arctic and Subarctic hydrography. *Earth System Science Data*, *10*(2), 1119–1138. https://doi.org/10.5194/essd-10-1119-2018

Berx, B., Hansen, B., Østerhus, S., Larsen, K. M., Sherwin, T., & Jochumsen, K. (2013). Combining in situ measurements and altimetry to estimate volume, heat and salt transport variability through the Faroe–Shetland Channel. *Ocean Science*, *9*(4), 639–654. https://doi.org/10.5194/os-9-639-2013

Boitsov, V. D., Karsakov, A. L., & Trofimov, A. G. (2012). Atlantic water temperature and climate in the Barents Sea, 2000-2009. *ICES Journal of Marine Science*, *69*(5), 833–840.

Borenäs, K. M., & Lundberg, P. A. (1988). On the deep-water flow through the Faore Bank Channel. *Journal of Geophysical Research*, *93*(C2), 1281–1292. https://doi.org/10.1029/JC093iC02p01281

Broecker, W. (1997). Thermohaline circulation, the Achilles heel of our climate system: Will man-made CO2 upset the current balance? *Science*, *278*, 1582–1588.

Buckley, M. W., & Marshall, J. (2016). Observations, inferences, and mechanisms of Atlantic Meridional overturning circulation variability: A review. *Reviews of Geophysics*, *54*, 5–63. https://doi.org/10.1002/2015RG000493

Cazenave, A., Palanisamy, H., & Ablain, M. (2018). Contemporary sea level changes from satellite altimetry: What have we learned? What are the new challenges? *Advances in Space Research*, *62*(7), 1639–1653. https://doi.org/10.1016/j.asr.2018.07.017

Chafik, L., Nilsen, J. E. Ø., Dangendorf, S., Reverdin, G., & Frederikse, T. (2019). North Atlantic Ocean circulation and decadal sea level change during the altimetry era. *Scientific Reports*, *9*(1), 1041. https://doi.org/10.1038/s41598-018-37603-6

Chafik, L., & Rossby, T. (2019). Volume, heat, and freshwater divergences in the subpolar North Atlantic suggest the Nordic Seas as key to the state of the meridional overturning circulation. *Geophysical Research Letters*, *46*, 4799–4808. https://doi.org/10.1029/2019GL082110

Childers, K. H., Flagg, C. N., Rossby, T., & Schrum, C. (2015). Directly measured currents and estimated transport pathways of Atlantic water between 59.5°N and the Iceland-Faroes-Scotland ridge. *Tellus A*, *67*(1), 28067. https://doi.org/10.3402/tellusa.v67.28067

Curry, W. B., & Oppo, D. W. (2005). Glacial water mass geometry and the distribution of $\delta^{13}C$ of ΣCO_2 in the western Atlantic Ocean. *Paleoceanography*, *20*, PA1017. https://doi.org/10.1029/2004PA001021

Dickson, B., Dye, S., Jónsson, S., Köhl, A., Macrander, A., Marnela, M., et al. (2008). The overflow flux west of Iceland: Variability, origins and forcing. In R. R. Dickson, et al. (Eds.), *ASOF—Arctic-Subarctic Ocean Fluxes*, (pp. 443–474). Berlin/Heidelberg, Germany: Springer. https://doi.org/10.1007/978-1-4020-6774-7_20

Dickson, R. R., Meincke, J., Malmberg, S.-A., & Lee, A. J. (1988). The "great salinity anomaly" in the northern North Atlantic 1968–82. *Progress in Oceanography*, *20*, 103–151.

Fofonoff, N. P. (1962). Dynamics of ocean currents. In M. N. Hill (Ed.), *The sea: Ideas and observations on progress in the study of the seas, Vol. 1, Physical oceanography* (pp. 323–395). New York: John Wiley & Sons.

Frajka-Williams, E., Beaulieu, C., & Duchez, A. (2017). Emerging negative Atlantic multidecadal oscillation index in spite of warm subtropics. *Scientific Reports*, *7*(1), 11224. https://doi.org/10.1038/s41598-017-11046-x

Hansen, B., Larsen, K. M. H., Hátún, H., Kristiansen, R., Mortensen, E., & Østerhus, S. (2015). Increasing transports of volume, heat, and salt towards the Arctic in the Faroe Current 1993–2013. *Ocean Science Discussions*, *12*(3), 1013–1050. www.ocean-sci-discuss.net/12/1013/doi:10.5194/osd-12-1013-2015

Hansen, B., Larsen, K. M. H., Hátún, H., & Østerhus, S. (2016). A stable Faroe Bank Channel overflow 1995–2015. *Ocean Science*, *12*, 1205–1220. https://doi.org/10.5194/os-12-1205-2016

Hansen, B., & Østerhus, S. (2000). North Atlantic–Nordic Seas exchanges. *Progress in Oceanography*, *45*(2), 109–208. https://doi.org/10.1016/S0079-6611(99)00052-X

Holliday, N. P., Cunningham, S. A., Johnson, C., Gary, S. F., Griffiths, C., Read, J. F., & Sherwin, T. (2015). Multidecadal variability of potential temperature, salinity, and transport in the eastern subpolar North Atlantic. *Journal of Geophysical Research: Oceans*, *120*, 5945–5967. https://doi.org/10.1002/2015JC010762

Jochumsen, K., Moritz, M., Nunes, N., Quadfasel, D., Larsen, K. M. H., Hansen, B., et al. (2017). Revised transport estimates of the Denmark Strait overflow. *Journal of Geophysical Research: Oceans*, *122*, 3434–3450. https://doi.org/10.1002/2017JC012803

Lozier, M. S., Li, F., Bacon, S., Bahr, F., Bower, A. S., Cunningham, S. A., et al. (2019). A sea change in our view of overturning in the subpolar North Atlantic. *Science*, *363*(6426), 516–521. https://doi.org/10.1126/science.aau6592

Mauritzen, C., Price, J., Sanford, T., & Torres, D. (2005). Circulation and mixing in the Faroese channels. *Deep Sea Research, Part I*, *52*(6), 883–913. https://doi.org/10.1016/j.dsr.2004.11.018

McManus, J. F., Francois, R., Gherardi, J.-M., Keigwin, L. D., & Brown-Leger, S. (2004). Collapse and rapid resumption of Atlantic meridional circulation linked to deglacial climate changes. *Nature*, *428*(6985), 834–837. https://doi.org/10.1038/nature02494

Østerhus, S., Woodgate, R., Valdimarsson, H., Turrell, B., de Steur, L., Quadfasel, D., et al. (2019). Arctic Mediterranean exchanges: A consistent volume budget and trends in transports from two decades of observations. *Ocean Science Discussions*, *15*(2), 379–399. https://doi.org/10.5194/os-15-379-2019

Palter, J. (2015). Role of the Gulf Stream in European climate. *Annual Review of Marine Science*, *7*(1), 113–137. https://doi.org/10.1146/annurev-marine-010814-015656

Rossby, T., Flagg, C., Chafik, L., Harden, B., & Søiland, H. (2018). A direct estimate of volume, heat and fresh water exchange across the Greenland-Iceland-Faroe-Scotland Ridge. *Journal of Geophysical Research: Oceans*, *123*, 7139–7153. https://doi.org/10.1029/2018JC014250

Segtnan, O. H., Furevik, T., & Jenkins, A. D. (2011). Heat and freshwater budgets of the Nordic Seas computed from atmospheric reanalysis and ocean observations. *Journal of Geophysical Research*, *116*, C11003. https://doi.org/10.1029/2011JC006939

Smedsrud, L. H., Esau, I., Ingvaldsen, R. B., Eldevik, T., Haugan, P. M., Li, C., et al. (2013). The role of the Barents Sea in the Arctic climate system. *Reviews Geophysics*, *51*, 415–449.

Taburet, G., Sanchez-Roman, A., Ballarotta, M., Pujol, M.-I., Legeais, J.-F., Fournier, F., et al. (2019). DUACS DT2018: 25 years of reprocessed sea level altimetry products. *Ocean Science*, *15*(5), 1207–1224. https://doi.org/10.5194/os-15-1207-2019

Trenberth, K. E., & Shea, D. J. (2006). Atlantic hurricanes and natural variability in 2005. *Geophysical Research Letters*, *33*, L12704. https://doi.org/10.1029/2006GL026894

van Oldenborg, G., te Raa, L., Dijkstra, H., & Philip, S. (2009). Frequency or amplitude dependent effects of the Atlantic meridional overturning on the tropical Pacific Ocean. *Ocean Science*, *5*(3), 293–301. https://doi.org/10.5194/os-5-293-2009

Wang, J., Yang, B., Charpentier Ljungqvist, F., Luterbacher, J., Osborn, T. J., Briffa, K. R., & Zorita, E. (2017). Internal and external forcing of multidecadal Atlantic climate variability over the past 1,200 years. *Nature Geoscience*, *10*(7), 512–517. https://doi.org/10.1038/NGEO2962

Whitehead, J. A. (1986). Flow of a homogeneous rotating fluid through straits. *Geophysical and Astrophysical Fluid Dynamics*, *36*(3-4), 187–205. https://doi.org/10.1080/03091928608210084

Zhang, R., Sutton, R., Danabasoglu, G., Kwon, Y.-O., Marsh, R., Yeager, S. G., et al. (2019). A review of the role of the Atlantic Meridional Overturning Circulation in Atlantic multidecadal variability and associated climate impacts. *Reviews of Geophysics*, *57*, 316–375. https://doi.org/10.1029/2019RG000644